



Predicting glass-forming compositions in the Al–La and Al–La–Ni systems

P. Gargarella^{a,*}, M.F. de Oliveira^b, C.S. Kiminami^c, S. Pauly^a, U. Kühn^a, C. Bolfarini^c, W.J. Botta^c, J. Eckert^{a,d}

^a IFW Dresden, Institut für Komplexe Materialien, Helmholtzstraße 20, D-01069, Dresden, Germany

^b Departamento de Engenharia de Materiais, Aeronáutica e Automobilística, Universidade de São Paulo, Av. Trabalhador Sancarlene, 400, 12560-970, São Carlos, São Paulo, Brazil

^c Departamento de Engenharia de Materiais, Universidade Federal de São Carlos, Rod. Washington Luis Km 235, 13565-905, São Carlos, Brazil

^d Institut für Werkstoffwissenschaft, Technische Universität Dresden, D-01062, Dresden, Germany

ARTICLE INFO

Article history:

Received 29 August 2010

Received in revised form

24 November 2010

Accepted 15 December 2010

Available online 23 December 2010

Keywords:

Glass forming ability

Metallic glasses

Amorphization criteria

Al–La–Ni system

ABSTRACT

In this work, a criterion considering the topological instability (λ) and the differences in the electronegativity of the constituent elements (Δe) was applied to the Al–La and Al–Ni–La systems in order to predict the best glass-forming compositions. The results were compared with literature data and with our own experimental data for the Al–La–Ni system. The alloy described in the literature as the best glass former in the Al–La system is located near the point with local maximum for the $\lambda \cdot \Delta e$ criterion. A good agreement was found between the predictions of the $\lambda \cdot \Delta e$ criterion and literature data in the Al–La–Ni system, with the region of the best glass-forming ability (GFA) and largest supercooled liquid region (ΔT_x) coinciding with the best compositional region for amorphization indicated by the $\lambda \cdot \Delta e$ criterion. Four new glassy compositions were found in the Al–La–Ni system, with the best predicted composition presenting the best glass-forming ability observed so far for this system. Although the $\lambda \cdot \Delta e$ criterion needs further refinements for completely describe the glass-forming ability in the Al–La and Al–La–Ni systems, the results demonstrated that this criterion is a good tool to predict new glass-forming compositions.

© 2010 Elsevier B.V. All rights reserved.

1. Introduction

Over the years, many parameters have been developed to characterize the ease of glass formation in metallic systems. Some of them are based on the thermal behaviour of the alloys, such as the reduced glass transition temperature, $T_{rg}(=T_g/T_l)$ [1], the extension of the supercooled liquid region, $\Delta T_x(=T_x - T_g)$ [2] and the γ_m parameter, $\gamma_m(=(2T_x - T_g)/T_l)$ [3] (where T_x is the crystallization temperature, T_l is the liquidus temperature and T_g is the glass transition temperature, respectively). Even though they are helpful in judging the glass-forming ability (GFA) of different compositions they fail in forecasting a priori the tendency of a metallic melt to vitrify as experimental data of the glass is required. Thus, trying to avoid the intensive laboratorial work and waste of material, which accompanies the trail-and-error approach, other parameters are required. In that respect, a very useful tool to select new compositions in multi-component systems are the empirical rules proposed by Johnson [4] and Inoue [2], nevertheless some exceptions are observed [5–13]. Other criteria based on the electronic structure [14], thermodynamic calculations [15,16], topological instability [17–20], differences in electronegativity [17] and structural mod-

els [15,21] have been proposed for identifying new metallic glasses. Especially the combination of some of these different parameters has been found to predict good glass-forming compositions even more reliably [15,17,22].

The topological instability criterion, also named λ criterion, was first proposed by Egami and Waseda [18] to determine the minimum solute concentration in a binary alloy system necessary to obtain an amorphous phase by rapid quenching. Sá Lisboa et al. [19] extended this criterion to describe the crystallization behaviour of Al-based alloys and Kiminami et al. [23] to predict new amorphous compositions. The λ values can be calculated using Eq. (1), where X_i is the atomic fraction of any solute element, Vm_i is the molar volume of any given solute and Vm_0 is the molar volume of the phase:

$$\lambda = \sum X_i \left| \frac{Vm_i}{Vm_0} - 1 \right| \quad (1)$$

The λ values indicate the level of destabilization of a crystalline host lattice with a given molar volume Vm_0 , which can be obtained with the insertion of new elements into this host phase. Therefore, the larger the λ value is, the larger the phase instability is and the easier glass formation becomes. Considering now one system with two adjacent phases: in the two phase region, there must be one point (composition) with maximum destabilization for both phases, where the λ values for the two phases coincide. These

* Corresponding author. Tel.: +49 3514659645.

E-mail address: p.gargarella@ifw-dresden.de (P. Gargarella).

points or “peaks” hence indicate the minimum λ value possible between them and an increased glass-forming ability is expected as a result of the maximum topological instability. This assumption is made considering all equilibrium phases, being possible to build a minimum λ plot [24].

Several works have stressed the influence of the electronegativity on the thermal behaviour of metallic glasses [25–27], which is related to the formation enthalpy (ΔH) [28] and the glass stability [29]. Therefore, it is reasonable to expect that the higher the average electronegativity difference among the elements is, the higher will be the glass-forming ability. Considering this, an average electronegativity map is built for the system of interest using Eq. (2):

$$\overline{\Delta e} = \sum X_i \left(\sum S_j |e_i - e_j| \right) \quad (2)$$

where $S_j = (X_j V m_j^{2/3}) / (\sum X_i V m_i^{2/3})$ and X_i and X_j are the atomic fractions of the atoms i and j , respectively, $V m_i$ and $V m_j$ are the molar volumes of the elements i and j , respectively and $e_i - e_j$ is the electronegativity difference between a central atom i and its j neighbours.

The λ and the Δe criterion are considered in a synergetic way leading to a final criterion map by multiplication of both criteria, resulting in the combined $\lambda \cdot \Delta e$ criterion.

Another criterion was proposed by Xi et al. [16] and it is based on the calculation of the γ^* parameter Eq. (3), that relates the formation enthalpy of amorphous and intermetallic phases, which can be calculated using the Miedema's model [30]. They considered only the contribution from enthalpies in their calculation, since the contribution from entropies is expected to be much smaller than the formation enthalpy of solids compounds. The driving force for glass formation ($-\Delta H^{\text{amor}}$) is related to the resistance of the glass against crystallization ($\Delta H^{\text{amor}} - \Delta H^{\text{inter}}$). Higher values of the γ^* parameter indicate larger GFA.

$$\gamma^* = \frac{-\Delta H^{\text{amor}}}{\Delta H^{\text{amor}} - \Delta H^{\text{inter}}} \quad (3)$$

where ΔH^{amor} and ΔH^{inter} are the formation enthalpies of the glass and the intermetallic compounds, respectively.

In this work, we calculated the $\lambda \cdot \Delta e$ criterion for the Al–La and Al–La–Ni system and compare the predictions for the glass-forming ability thus obtained with literature data and our own experimental data. Furthermore, a comparison between this criterion and the γ^* criterion is made for the Al–La system.

2. Experimental procedure

The calculations of the $\lambda \cdot \Delta e$ criterion were done for the Al–La and Al–La–Ni systems using Eqs. (1) and (2). The γ^* parameter was also calculated for the Al–La system using Eq. (3). Five compositions in the Al–La–Ni system indicated as alloys with high glass-forming ability were selected to be studied: $\text{La}_{56}\text{Al}_{26.5}\text{Ni}_{17.5}$ (the best composition predicted with the highest $\lambda \cdot \Delta e$ value), $\text{Ni}_{75}\text{La}_{11}\text{Al}_{14}$, $\text{Al}_{41}\text{La}_{36}\text{Ni}_{23}$, $\text{La}_{65}\text{Al}_{17.5}\text{Ni}_{17.5}$, and $\text{La}_{55.5}\text{Al}_{19.5}\text{Ni}_{25}$.

Ingot of these compositions were prepared by arc-melting using elements with high purity (more than 99.5% purity). They were repeatedly arc-melted in an argon atmosphere to ensure complete melting and compositional homogeneity. The surface of the elements Al and Ni was chemically cleaned and the pieces of La (small blocks) were ground before the experiments.

Ribbons were produced using a single-roller melt-spinner with a tangential wheel speed of 42 m/s under argon atmosphere. The approximate width and thickness of the melt-spun ribbons were 3 mm and 35 μm , respectively.

The structure of these ribbons was characterized using a Siemens D5005 X-ray diffractometer (XRD) in reflection mode using Cu-K α radiation, and the thermal stability was studied by differential scanning calorimetry (DSC) at a heating rate of 40 K/min in a Netzsch STA 449C.

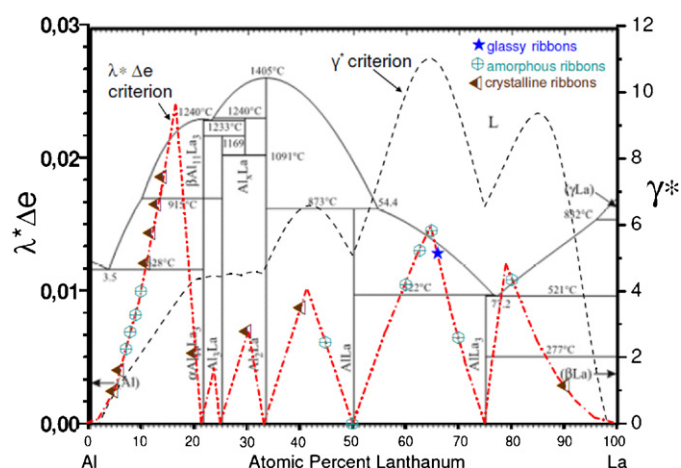


Fig. 1. Schematic figure with the results for the $\lambda \cdot \Delta e$ (dashed dotted line) and γ^* (dashed line) criteria applied to the Al–La system. Larger values indicate higher glass-forming ability. The binary phase diagram [34] and the literature data [31–33] are also shown for comparisons.

3. Results and discussion

3.1. Al–La system

The results for the $\lambda \cdot \Delta e$ criterion are indicated in Fig. 1 together with literature data for the binary Al–La system [31–33]. The binary phase diagram [34] and the results for the γ^* criterion [16] are also plotted for comparison. Larger values for the $\lambda \cdot \Delta e$ and γ^* criteria indicate binary compositions with a relatively high glass-forming ability.

All the literature data plotted here were obtained from ribbons and their thermal behaviour were verified using DSC at heating rate of 30 K/min for the $\text{La}_{63}\text{Al}_{37}$, $\text{La}_{65}\text{Al}_{35}$ and $\text{La}_{66}\text{Al}_{34}$ alloys [33] and of 40 K/min for the other alloys [31,32]. We can verify that only one glassy alloy was found in this system, viz. $\text{La}_{66}\text{Al}_{34}$, and this composition is located very close to the peak around 65% at. La in the $\lambda \cdot \Delta e$ curve (Fig. 1). Also a good agreement is obvious between the $\lambda \cdot \Delta e$ and the γ^* criterion, since both yield three similar peaks on the La-rich side of the phase diagram.

The peak observed in the $\lambda \cdot \Delta e$ curve near the Al–solid solution (17 at.% La) does not properly describe the glass-forming range. Many works showed that the best region of amorphization near the Al–solid solution is around the point $\lambda = 0.1$ for Al–TM–RE systems [18,19,27,35]. In the case of the Al–La system the $\lambda = 0.1$ point, calculated using Eq. (1), corresponds to $\text{Al}_{92}\text{La}_8$, which is in agreement with the range of amorphous formation verified in the literature [31] and indicated in Fig. 1. We suppose that the reason for this behaviour is the most efficient packing of the different types of clusters obtained for compositions around this point [35–37] that favour the supercooled liquid stability, improving the glass-forming ability.

Only crystalline ribbons could be prepared for the composition near the two smaller peaks of the $\lambda \cdot \Delta e$ curve around 30 and 41 at.% La. One possible reason for this might be the relatively high liquidus temperature of these alloys (1653 and 1603 K, respectively; more than two times the eutectic temperature in the La-rich side, 794 K), indicating a low stability of the liquid in this compositional range. The liquidus temperature profile needs to be considered as one indicator before the selection of the alloys.

It is important to point out here that the calculation of the γ^* parameter is complicated (many approximation are made) and can be attained only for binary [38,39] and ternary systems [40]. On the other hand, the calculation of the $\lambda \cdot \Delta e$ criterion is easier and can be carried out for more than 3 elements. This criterion is

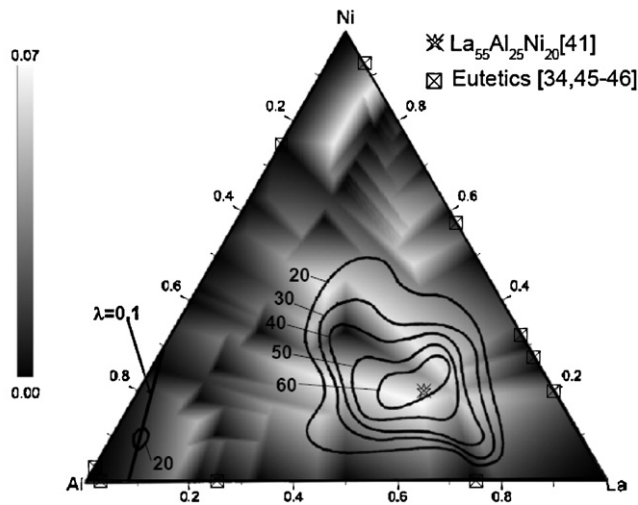


Fig. 2. The final $\lambda \cdot \Delta e$ criterion map in comparison with literature data [32,41] and eutectic compositions [34,45,46]. The maximum value for the criterion is indicated by the scale beside the graph; higher values are represented by brighter regions that indicate compositional regions with high glass-forming ability. The circles indicate ΔT_x regions found experimentally by Inoue et al. [32].

limited because considers by definition that intermetallic compositions present the same glass-forming ability, what is not verified experimentally [8].

3.2. Al–La–Ni system

Fig. 2 presents the results for the $\lambda \cdot \Delta e$ criterion applied to the Al–La–Ni system together with literature data [32,41]. The brightest spots indicate compositions with the highest $\lambda \cdot \Delta e$ value. The $\text{La}_{55}\text{Al}_{25}\text{Ni}_{20}$ alloy [41] is reported to be the best glass former in this system with a critical diameter of 3 mm and it is located very close to the composition with the maximum value for the $\lambda \cdot \Delta e$ criterion ($\text{La}_{56}\text{Al}_{26.5}\text{Ni}_{17.5}$). Regions of ΔT_x have been measured by Inoue et al. [32] and the extension of the supercooled liquid region increases in the direction of the maximum $\lambda \cdot \Delta e$ values as shown in **Fig. 2**. This trend is expected if one assumes that the ΔT_x values are directly proportional to the glass-forming ability. A large value for ΔT_x indicates that the supercooled liquid can span over a wide temperature range without crystallization and hence has a high resistance against nucleation and growth of crystalline phases [42,43]. Additionally, **Fig. 2** shows that the region with best glass-forming ability in the Al-rich corner [32,44] is located on the $\lambda = 0.1$ line as was mentioned before.

The compositions selected to check the reliability of the GFA prediction by the $\lambda \cdot \Delta e$ criterion are indicated in **Fig. 3** together with the binary eutectic compositions [34,45,46]. The XRD results for the ribbons produced by melt-spinning are displayed in **Fig. 4**. Only $\text{Ni}_{75}\text{La}_{11}\text{Al}_{14}$ shows a fully crystalline structure, and the others exhibit two broad maxima characteristic of an amorphous structure, with only some small sharp crystalline peaks of relative low intensity being superimposed. These peaks could not be identified unambiguously but exhibit some similarity in the 2θ positions, which indicates that they might be related to the same crystalline phase. Considering that these compositions are located in different compositional regions suggests that these peaks could correspond to some complex oxide(s).

The DSC curves obtained for the ribbons are shown in **Fig. 5** and the results combined with the values for ΔT_x , T_{rg} and the γ_m parameter are summarized in **Table 1**. The curve for the $\text{La}_{11}\text{Al}_{14}\text{Ni}_{75}$ alloy is not showed in **Fig. 5** because no crystallization peak was observed. The maximum ΔT_x , T_{rg} and γ_m values are obtained for

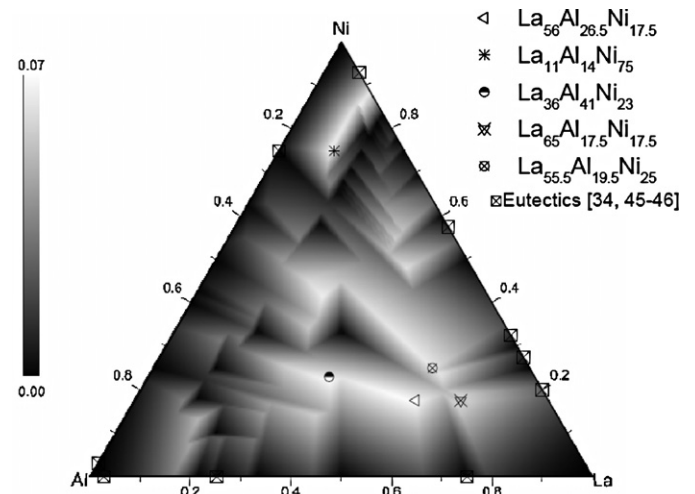


Fig. 3. The final $\lambda \cdot \Delta e$ criterion map for the Al–La–Ni system with the selected compositions. The binary eutectic compositions [34,45,46] are also indicated.

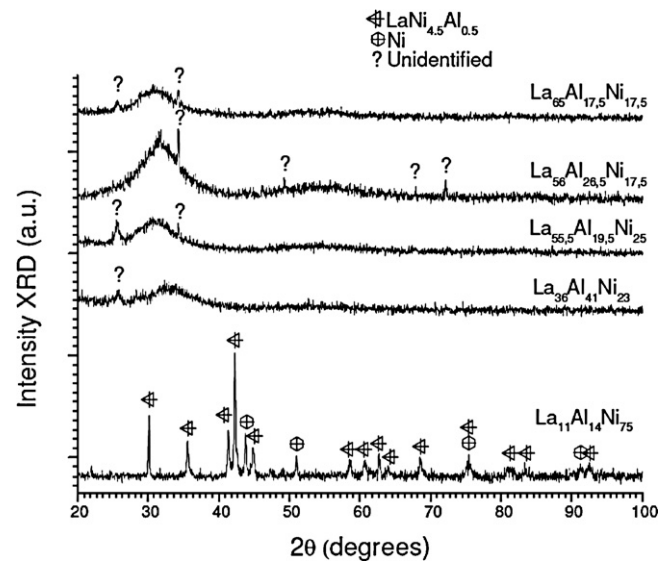


Fig. 4. XRD results for the ribbons of the selected compositions.

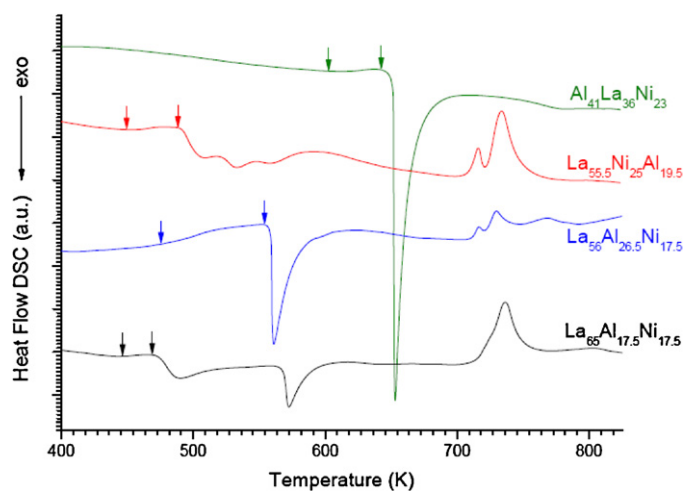


Fig. 5. DSC results for the ribbons analysed using heating rate of 40K/min (the curve for the $\text{La}_{11}\text{Al}_{14}\text{Ni}_{75}$ alloy is not showed because no crystallization peak was observed). The arrows indicate the glass transition temperature (T_g) and the crystallization temperature (T_x), respectively.

Table 1

Results of the DSC analysis for the ribbons at heating rate of 40 K/min. T_g and T_x were defined as onset temperatures and $T_{rg} = T_g/T_1$ [1], $\Delta T_x = T_x - T_g$ [2] and $\gamma_m = (2T_x - T_g)/T_1$ [3].

Alloys	T_g (K)	T_x (K)	ΔT_x (K)	T_1 (K)	T_{rg}	γ_m	$\lambda \cdot \Delta e$
La ₆₅ Al _{17.5} Ni _{17.5}	446 ± 2	468 ± 2	22 ± 2	821 ± 2	0.54	0.60	0.053
La ₅₆ Al _{26.5} Ni _{17.5}	475 ± 2	554 ± 2	79 ± 2	798 ± 2	0.59	0.79	0.069
La _{55.5} Al _{19.5} Ni ₂₅	450 ± 2	487 ± 2	37 ± 2	813 ± 2	0.55	0.64	0.064
La ₃₆ Al ₄₁ Ni ₂₃	603 ± 2	642 ± 2	39 ± 2	1276 ± 2	0.47	0.53	0.064
La ₁₁ Al ₁₄ Ni ₇₅	–	–	–	1566 ± 2	–	–	0.058

the La₅₆Al_{26.5}Ni_{17.5} alloy, which at the same time presents the highest value for the $\lambda \cdot \Delta e$ criterion. The values for ΔT_x , T_{rg} and γ_m were 79 K, 0.59 and 0.79, respectively, and they are the highest measured so far for this system. All the other alloys present relatively high values for the combined $\lambda \cdot \Delta e$ criterion, exhibiting a distinct correlation with the ΔT_x values. Yet, despite this obvious agreement of the supercooled liquid region and the $\lambda \cdot \Delta e$ value, a clear trend between the $\lambda \cdot \Delta e$ values and T_{rg} and the γ_m parameter cannot be established. The La₃₆Al₄₁Ni₂₃ alloy exhibits a relatively high value for the $\lambda \cdot \Delta e$ criterion (0.064) compared to the other alloys studied in this work but it exhibits low values for the T_{rg} and γ_m with 0.47 and 0.53, respectively.

On the Ni-rich side of the ternary phase diagram, La₁₁Al₁₄Ni₇₅ has a relatively high value for the combined criterion (0.058) but does not exhibit any glass transition or crystallization peak during the DSC run and consequently is fully crystalline as XRD additionally proves (Fig. 4). This discrepancy is due to the fact that this composition is located near solid solution region, where the combined $\lambda \cdot \Delta e$ criterion is not effective as discussed before. Another point is that the Ni solid solution region presents very high liquid temperatures (T_1), as was indicated for this alloy with T_1 of 1566 K and can be verified in the binary phase diagrams [45,46]. This indicates low liquid stability, i.e. low glass-forming ability.

Proportionality between the $\lambda \cdot \Delta e$ criterion and the ΔT_x values was verified by examining the literature and experimental data, with larger values indicating wider supercooled liquid region windows. A similar relation between ΔT_x values and the factors considered in the $\lambda \cdot \Delta e$ criterion, namely the electronegativity difference and the atomic size was reported by Fang et al. [47]. They showed that ΔT_x values are proportional to these two factors and furthermore to the valence electron difference, with a good correlation being established between calculated and experimental ΔT_x values for Fe-, Pd- and Mg-based alloys [29,47]. Considering that the larger the ΔT_x value the higher the critical diameter for amorphization, one can conclude that the La₅₆Al_{26.5}Ni_{17.5} alloy possesses the highest GFA in this system. This agrees well with previous reports for Al–La–Ni and Al–La–(Ni, Cu) alloys in the literature [32,41,43].

4. Conclusions

The compositional regions indicated by the $\lambda \cdot \Delta e$ criterion as good glass-forming regions in the Al–La and Al–La–Ni systems coincide with the best glass formers verified in the literature and in the current experiments.

New glass-forming compositions were found in the Al–La–Ni system and a clear correlation between ΔT_x and the $\lambda \cdot \Delta e$ values was verified. The La₅₆Al_{26.5}Ni_{17.5} alloy presents the highest ΔT_x , T_{rg} and γ_m found for this system so far.

Although the $\lambda \cdot \Delta e$ criterion could predict the best glass formers verified in the Al–La and Al–La–Ni systems, the results demonstrated that it can not be considered alone to describe the GFA in these systems. Considerations as liquidus temperature profile and the cluster formation need also to take into account.

Acknowledgments

The authors thank S. Donath, M. Frey and U. Wilke for technical assistance, and K. Song, N.S. Barekar and C.R. Aliaga for stimulating discussions. Financial support granted by FAPESP, CAPES, CNPq (Brazil) and DAAD (Germany) is gratefully acknowledged.

References

- [1] D. Turnbull, *Contemporary Physics* 10 (1969) 473–488.
- [2] A. Inoue, *Acta Materialia* 48 (2000) 279–306.
- [3] S. Guo, Z.P. Lu, C.T. Liu, *Intermetallics* 18 (2010) 883–888.
- [4] W.L. Johnson, *MRS Bulletin* 24 (1999) 42–56.
- [5] F.Q. Guo, S.J. Poon, G.J. Shiflet, *Applied Physics Letters* 84 (2004) 37–39.
- [6] Y. Ke-Fu, R. Fang, *Chinese Physics Letters* 22 (2005) 1481–1483.
- [7] K.J. Laws, K.F. Shamlaye, B. Gun, M. Ferry, *Journal of Alloys and Compound* 486 (2009) L27–L29.
- [8] T. Mei-Bo, Z. De-Quian, P. Ming-Xiang, W. Wei-Hua, *Chinese Physics Letters* 21 (2004) 901–903.
- [9] E.S. Park, D.H. Kim, *Acta Materialia* 54 (2006) 2597–2604.
- [10] B.A. Sun, M.X. Pan, D.Q. Zhao, W.H. Wang, X.K. Xi, M.T. Sandor, Y. Wu, *Scripta Materialia* 59 (2008) 1159–1162.
- [11] Y. Wang, Q. Wang, J. Zhao, C. Dong, *Scripta Materialia* 63 (2010) 178–180.
- [12] L. Xia, S.T. Shan, D. Ding, Y.D. Dong, *Intermetallics* 15 (2007) 1046–1049.
- [13] B. Zhang, D.Q. Zhao, M.X. Pan, R.J. Wang, W.H. Wang, *Acta Materialia* 54 (2006) 3025–3032.
- [14] Q. Jiang, B.Q. Chi, J.C. Li, *Applied Physics Letters* 82 (2003) 2984–2986.
- [15] J. Cheney, H. Khalifa, K. Vecchio, *Materials Science and Engineering A* 506 (2009) 94–100.
- [16] L. Xia, S.S. Fang, Q. Wang, Y.D. Dong, C.T. Liu, *Applied Physics Letters* 88 (2006) 171903–171905.
- [17] M.F. de Oliveira, F.S. Pereira, C. Bolfarini, C.S. Kiminami, W.J. Botta, *Intermetallics* 17 (2009) 183–185.
- [18] T. Egami, Y. Waseda, *Journal of Non-Crystalline Solids* 64 (1984) 113–134.
- [19] R.D.S. Lisboa, C. Bolfarini, F. W.J.B., C.S. Kiminami, *Applied Physics Letters* 86 (2005) 211903–211904.
- [20] D.B. Miracle, O.N. Senkov, *Materials Science and Engineering A* 347 (2003) 50–58.
- [21] D.B. Miracle, *Natural Materials* 3 (2004) 697–702.
- [22] B. Yang, Y. Du, Y. Liu, *Transactions of Nonferrous Metals Society of China* 19 (2009) 78–84.
- [23] C.S. Kiminami, R.D. Sá Lisboa, M.F. de Oliveira, C. Bolfarini, W.J. Botta, *Materials Transactions JIM* 48 (2007) 1739–1742.
- [24] W.J. Botta, F.S. Pereira, C. Bolfarini, C.S. Kiminami, M.F. de Oliveira, *Philosophical Magazine* 88 (2008) 785–791.
- [25] D.V. Louzguine, A. Inoue, *Applied Physics Letters* 79 (2001) 3410–3412.
- [26] D.V. Louzguine-Luzgin, A. Inoue, W.J. Botta, *Applied Physics Letters* 88 (2006) 011911–011913.
- [27] C.S. Ma, J. Zhang, X.C. Chang, W.L. Hou, J.Q. Wang, *Philosophical Magazine Letters* 88 (2008) 917–924.
- [28] S. Fang, Z. Zhou, J. Zhang, M. Yao, F. Feng, D.O. Northwood, *Journal of Alloys and Compound* 293–295 (1999) 10–13.
- [29] S. Fang, X. Xiao, L. Xia, W. Li, Y. Dong, *Journal of Non-Crystalline Solids* 321 (2003) 120–125.
- [30] A.R. Miedema, P.F. de Châtel, F.R. de Boer, *Physica* 100B (1980) 1–28.
- [31] A. Inoue, K. Ohtera, T. Masumoto, *Japanese Journal of Applied Physics* 27 (1988) L736–L739.
- [32] A. Inoue, T. Zhang, T. Masumoto, *Materials Transactions JIM* 30 (1989) 965–972.
- [33] P. Gargarella, C.S. Kiminami, M.F. de Oliveira, C. Bolfarini, W.J. Botta, *Materials Science and Engineering A* 512 (2009) 53–57.
- [34] H. Okamoto, *Journal of Phase Equilibria and Diffusion* 28 (2007) 581.
- [35] P. Gargarella, C.S. Kiminami, M.F. de Oliveira, C. Bolfarini, W.J. Botta, *Journal of Alloys and Compound* 495 (2010) 334–337.
- [36] W.J. Botta, C.T. Rios, R.D. Sá Lisboa, A.R. de Andrade, M.F. de Oliveira, C. Bolfarini, C.S. Kiminami, *Journal of Alloys and Compound* 483 (2009) 89–93.
- [37] D.B. Miracle, O.N. Senkov, *Journal of Non-Crystalline Solids* 319 (2003) 174–191.
- [38] L. Xia, D. Ding, S.T. Shan, Y.D. Dong, *Journal of Physics: Condensed Matter* 18 (2006) 3543–3548.

- [39] L. Xia, W.H. Li, S.S. Fang, B.C. Wei, Y.D. Dong, *Journal of Applied Physics* 99 (2006) 026103.
- [40] M.F. de Oliveira, L.C.R. Aliaga, C. Bolfarini, W.J. Botta, C.S. Kiminami, *Journal of Alloys and Compound* 464 (2008) 118–121.
- [41] A. Inoue, T. Nakamura, T. Sugita, T. Zhang, T. Masumoto, *Materials Transactions JIM* 34 (1993) 351–358.
- [42] A. Inoue, T. Zhang, T. Masumoto, *Materials Transactions JIM* 31 (1990) 177–183.
- [43] A. Inoue, H. Yamaguchi, T. Zhang, T. Masumoto, *Materials Transactions JIM* 31 (1990) 104–109.
- [44] W.S. Sanders, J.S. Warner, D.B. Miracle, *Intermetallics* 14 (2006) 348–351.
- [45] B. Predel, in: O. Madelung (Ed.), *Al–Ni (Aluminum–Nickel)*, Landolt–Börnstein – Group IV Physical Chemistry Numerical Data and Functional Relationships in Science and Technology, 1991.
- [46] B. Predel, in: O. Madelung (Ed.), *La–Ni (Lanthanum–Nickel)*, Landolt–Börnstein – Group IV Physical Chemistry Numerical Data and Functional Relationships in Science and Technology, 1997.
- [47] S. Fang, X. Xiao, L. Xia, Q. Wang, W. Li, Y. Dong, *Intermetallics* 12 (2004) 1069–1072.